



Genesis and propagation of exogenous sediment pulses in mountain channels: insights from flume experiments with seismic monitoring

Marco Piantini^{1,2}, Florent Gimbert¹, Hervé Bellot², Alain Recking²

5 ¹ University Grenoble Alpes, CNRS, IRD, Institute for Geosciences and Environmental Research (IGE), Grenoble, France

² University Grenoble Alpes, INRAE, ETNA, Grenoble, France

Correspondence to: Marco Piantini (marco.piantini@univ-grenoble-alpes.fr)

Abstract. In the upper part of mountain river catchments, large amounts of loose debris produced by mass wasting processes
10 can accumulate at the base of slopes and cliffs. Sudden destabilizations of these deposits are thought to trigger energetic
sediment pulses that may travel in downstream rivers with little exchange with the local bed. The dynamics of these exogenous
sediment pulses remain poorly known because direct field observations are lacking, and the processes that control their
formation and propagation have rarely been explored experimentally.

Here we carry out flume experiments with the aims of investigating (i) the role of sediment accumulation zones in the
15 generation of sediment pulses, (ii) their propagation dynamics in low-order mountain channels, and (iii) the capability of
seismic methods to unravel their physical properties. We use an original set-up where we supply with liquid and solid discharge
a low slope storage zone acting like a natural sediment accumulation zone, and connected to a downstream 18 % steep channel
equipped with geophones.

We show that the ability of the self-formed deposit to generate sediment pulses depends on the sand content of the mixture. In
20 particular, when a high fraction of sand is present, the storage area experiences alternating phases of aggradation and erosion
strongly impacted by grain sorting. The upstream processes also influence the composition of the sediment pulses, which are
formed by a front made of the coarsest fraction of the sediment mixture, a body composed of a high concentration of sand
corresponding to the peak of solid discharge, and a diluted tail that exhibits a wide grain size distribution. Seismic
measurements reveal that the front dominates the overall seismic noise, but we observe a complex dependency between seismic
25 power and sediment pulses' transport characteristics, which questions the applicability of existing simplified theories in such
context.

These findings challenge the classical approach for which the sediment budget of mountain catchments is merely reduced to
an available volume, since not only hydrological but also granular conditions should be considered to predict the occurrence
and propagation of such sediment pulses.

30



1 Introduction

Sediment transport processes play a key role in fluvial geomorphology (Schumm, 2003) and natural risk management (Badoux et al., 2014), since they exert a major control in the intensity with which rivers can impact the landscape and the safety of inhabited regions. This is particularly evident in mountain catchments, where catastrophic floods are exacerbated by a rapid hydrological response to rainfall (high hydrological connectivity, (Wohl, 2010)) and a large mobilization of sediments (Recking, 2014). Predicting when and how sediments move throughout mountain channels, however, remains challenging since onset of motion criteria and bedload transport laws have mostly been established for lowland rivers and have limited applicability to mountain environments (Schneider et al., 2016). Mountain rivers are characterized by a wide range of morphological units whose peculiarities cannot be neglected when predicting sediment load (Lee and Ferguson, 2002; Comiti et al., 2009; Zimmermann et al., 2010). For instance, several works have shown that large-scale bed roughness are expected to affect bed shear stress (Solari and Parker, 2000; Lamb et al., 2008; Recking, 2009; Prancevic and Lamb, 2015), and grain sorting processes have a stronger impact in producing bedload fluctuations compared to lowland streams (Recking et al., 2009; Bacchi et al., 2014). Moreover, the steepness of mountain channels may help trigger debris flows, which are energetic transport processes where the sediment concentration is so high (greater than 50 % by volume) that the solid phase influences the behaviour of the flow as much as the fluid phase (Iverson, 1997). The conditions of transition from bedload to debris flow remains debated partly due to lacking field observations (Mao et al., 2009; Prancevic et al., 2014).

For both fluvial and debris flows processes, in addition to the hydrological forcing, sediment supply conditions play an important role (Benda and Dunne, 1997; Bovis and Jakob, 1999; Recking, 2012) and their spatial and temporal variabilities add complexity to predictions. Mountain channels that are coupled to sediment production zones (high landscape connectivity, (Wohl, 2010)) are particularly prone to receive episodic inputs of material coming from deposits fed by mass wasting processes and destabilized by rainfalls and runoff descending from upstream rocky channels. This is for example the case in the Roize River, France (Fig. 1a). The upper part of the catchment is characterized by cliffs producing large amount of debris that accumulate at the slope's toe (Fig. 1b and (Lamand et al., 2017)), and as a result of hydrological and gravitational phenomena, sediments are occasionally released to the coupled reach (Fig. 1c) where they are transported downstream to a reception zone (sediment trap).

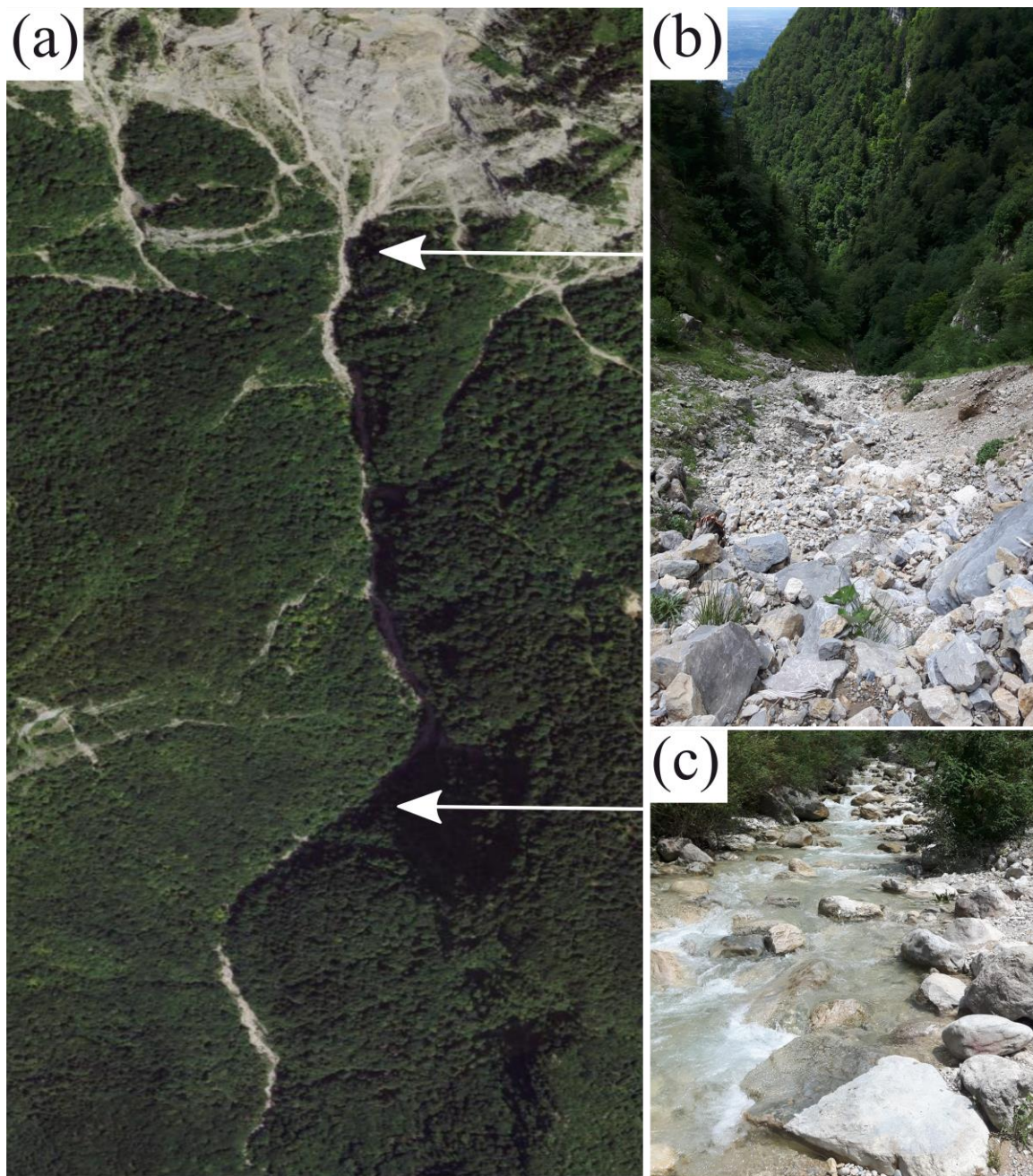


Figure 1: (a) A typical mountain stream configuration (the Roize River, <https://www.geoportail.gouv.fr>) with: (b) a production zone (sediments deposits are several meters thick and show evidences of large incisions) and (c) a transfer zone consisting in a narrow steep step-pool morphology.

60 Several works have shown that exogenous sediment inputs in a river usually take the form of *sediment pulses*, defined in the literature as disturbances in bed elevation that propagate downstream translating as a coherent wave end/or dispersing in place (Sutherland et al., 2002; Brummer and Montgomery, 2006). Almost all the studies (Lisle et al., 1997; Sutherland et al., 2002;



Cui et al., 2003; Cui and Parker, 2005; Sklar et al., 2009) have investigated the evolution of these sediment pulses in gravel-bed rivers characterized by a maximum slope of 1 %, where the streambed has been shown to actively interact with the injected
65 material. However, since low-order rivers usually present geological controls such as rarely mobile boulders and bedrock outcrops, as well as much steeper slope, sediment pulses are expected to be transported downstream with a marginal morphological impact on the underlying bed, following the “travelling bedload” concept (Piton and Recking, 2017). Thanks to these exogenous inputs of sediments, such streams can suddenly switch from supply limited to overcapacity conditions, as illustrated in Fig. 2 where the non-alluvial and inactive bed of the Ruisseau de la Gorge (French Alps) suddenly experienced
70 a large transport event in 2015. As the transported sediments were much finer than the bed in place, an upstream and exogenous input of the material was suggested. To the best of our knowledge, there are no experimental studies that investigate sediment pulses’ propagation in such configuration, and direct field observations are also lacking. Classical monitoring methods reveal scarce effectiveness for impulsive events (Mao et al., 2009), and therefore sediment pulses are challenging to track due to their localized and potentially energetic nature. In this context, seismic methods represent a robust alternative for providing a non-
75 invasive and continuous monitoring of torrential processes (Burtin et al., 2016) and catastrophic floods (Cook et al., 2018). As sediment transport generates ground vibrations, mechanistic models have been defined to invert seismic measurements into river process properties such as sediment flux, grain size and impact rates (Tsai et al., 2012; Lai et al., 2018; Farin et al., 2019). Recent works have demonstrated applicability of these frameworks for bedload in the laboratory (Gimbert et al., 2019) and in the field (Bakker et al., 2020) under relatively low transport rates, however the extent to which they continue to apply to flows
80 like sediment pulses remains to be investigated.



Figure 2: Effect of a sediment pulse at a bridge section of the Gorges river (France), a stream that was known by local engineers for having been inactive for decades. The transported material was much finer ($D_{50} = 96 \text{ mm}$, $D_{84} = 169 \text{ mm}$) than the bed in place ($D_{50} = 250 \text{ mm}$, $D_{84} = 413 \text{ mm}$).

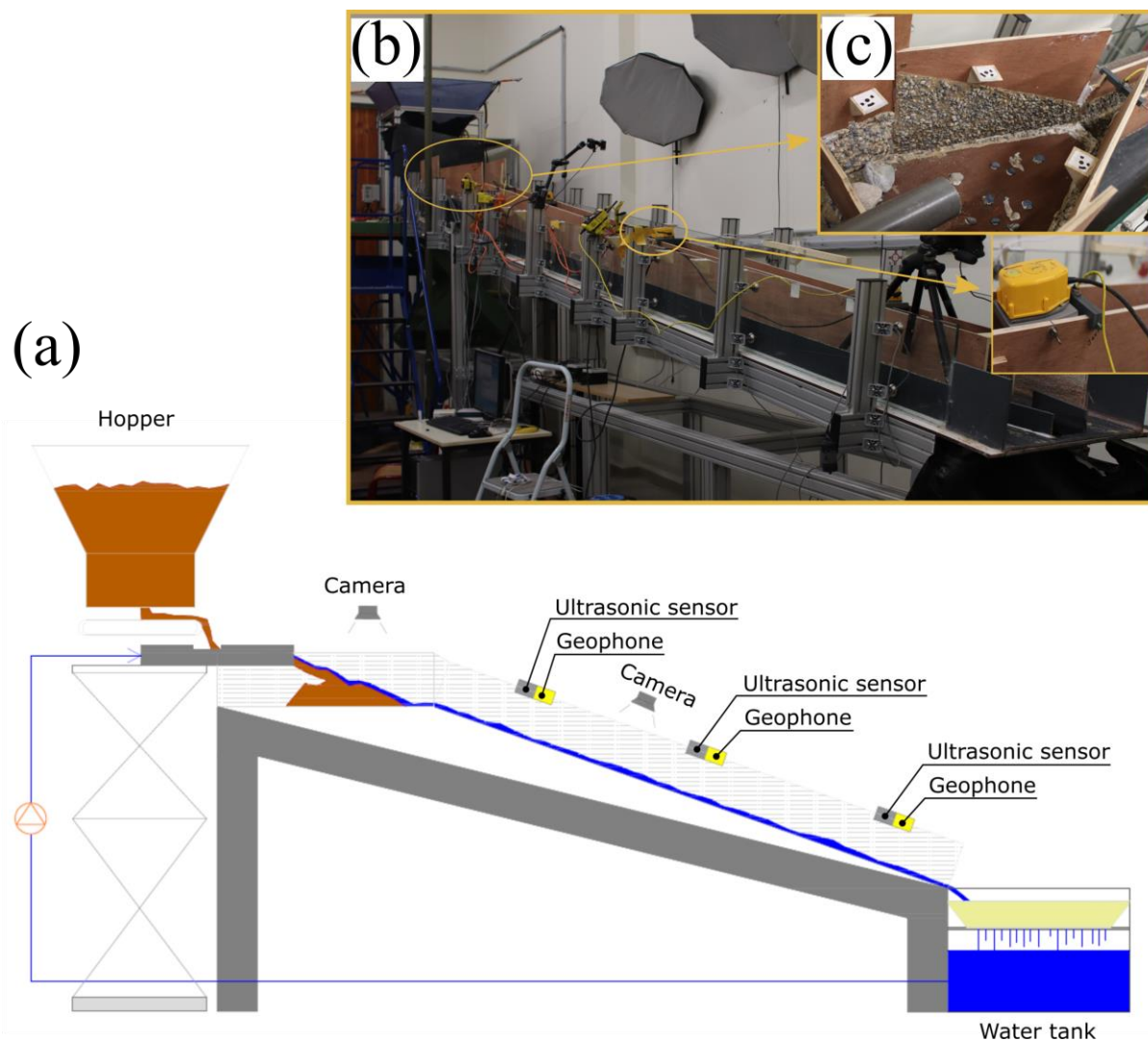


85 In this study we conduct laboratory experiments (i) to explore the role of sediment accumulation zones in the generation of
sediment pulses, (ii) to investigate their propagation dynamics in low-order mountain channels, and (iii) to test the capability
of seismic methods to infer the flow properties associated to such sediment transport events. We use an original set-up where
instead of feeding the flume section directly as usually done, we supply with liquid and solid discharge a low slope storage
zone connected to the upstream part of a 18 % steep channel. Such an experimental configuration allows us to investigate if a
90 self-formed deposit can generate sediment pulses and how these later propagate in the downstream channel. In *Sect. 2* we
present the experimental set-up and the measurements protocol. Then in *Sect. 3* we present our experimental results regarding
both the storage area and the channel. Finally, in *Sect. 4* we discuss the key results and we describe the main implications for
mountain stream morphodynamics.

2 Material and methods

95 2.1 Experimental set-up and measurements

We use a 6 m long flume made of (i) a 1 m long and on average 0.5 m wide trapezoidal shaped upstream storage area and (ii)
a 5 m long and 0.1 m wide downstream steep (18 % slope) channel (Fig. 3).



100 **Figure 3: Panel (a): scheme of the flume with the instrumental equipment; panel (b): a photo of the flume; panel (c): a zoom on (i)**
105 **the upstream storage area and (ii) one of the three sections equipped with a geophone (yellow device) and an ultrasonic sensor (grey**
housing).

In order to reproduce the immobile natural roughness of steep torrents, the bed and the side walls of the flume are made of
glued sediments of maximum diameter 6.3 mm. The width is calculated to have a channel width/surface—grain-size ratio
105 lower than 10, referring to the definition of steep “small channels” (Comiti and Mao, 2012).

Water discharge recirculation is ensured by a pump supplied by a reservoir placed at the flume outlet, whose level is kept
constant through an overflow drain. The discharge value is measured with an electromagnetic flowmeter and the flow rate is
controlled numerically using a calibrated voltage/discharge relationship. We use a sediment feeding system composed of a
hopper connected to a conveyor belt for the solid discharge. The sediment flux is controlled by the velocity of the conveyor



110 belt which is measured by a sensor fixed on one of its rotation axes. As for the water supply we set a calibrated equation in order to regulate the solid discharge through the computer.

The topographic evolution of the storage area is monitored with a sensing camera (Microsoft Kinect) that allows to reproduce a virtual 3-D model from the images through depth-sensing techniques: a light is firstly projected by an infrared sensor, then the reflected pattern is captured to recover the geometry of the object by computing the light's time of flight. The device is
115 used to estimate the volume variation of the deposit and its longitudinal slope.

We video record each experiment with two webcams placed at the inlet section and along the channel (Microsoft HD LifeCam Cinema). Three sections are equipped with a remote transducer ultrasonic sensor (Banner Q45UR Series) and a geophone (3-D Geophone PE-6/B) (Fig. 3) to respectively measure the flow stage and detect flow-induced seismic flume motion generated by particle impacts (Govi et al., 1993). The data from the geophones are recorded on a DATA-CUBE³ logger with a sampling
120 frequency of 800 Hz. In order to explore the properties of the seismic noise, we compute the power spectral density (PSD) of the signal recorded along the vertical by performing a fast Fourier transform with the Welch's averaging method (Welch, 1967). According to this method the time series is split into overlapping segments (here we chose an overlap of 50 %), and the final PSD results from the average over the PSDs of each segment. We focus on sediment transport-related seismic noise by getting rid of other sources emitted by the experimental device (e.g. water pump, water flow in pipes and on the flume,
125 etc..) through normalizing the raw signal by the seismic power occurring under similar experimental conditions but with no sediment transport (see *Sect. S2* in Supplement). We measure the sediment flux by sampling the outgoing sediments at the channel exit and we compute the grain size distribution of the samples from sieve measurements. It is worth noting that solid discharge is measured by hand and is consequently not continuous in time, and the sampling frequency is adapted to flow conditions. As flow stage and seismic noise are monitored at a different section than the outlet solid discharge, a time lag
130 between measurements is present. In order to compute the expected temporal delay and to properly compare the measured data, we time shift the outlet solid discharge by estimating the velocity of the flux with a cross correlation between the three flow stage time series. Such a time-shift procedure is appropriate for the seismic analysis thanks to significant signal amplification (+ 5 dB in average) occurring near the geophone in our experimental setting (see *Sect. S4* in Supplement).

2.2 Experimental input conditions

135 Several experiments are carried out varying the grain size distribution of the mixture. We account for grain size heterogeneity through using a sediment mixture characterized by a bimodal grain size distribution, with the two modes corresponding to sand ($0.5 \text{ mm} < D < 2 \text{ mm}$) and cobbles ($4 \text{ mm} < D < 8 \text{ mm}$) (Main experiment in Table I and Fig. 4). The poorly sorted mixture is obtained with respect to grain size distribution utilized in previous experimental works on steep slope (Bacchi et al., 2014) and is characterized by $D_{50} = 5.16 \text{ mm}$ and $D_{84} = 9 \text{ mm}$, where D_X is the X th percentile particle diameter. In addition
140 to this sediment mixture, we also test another bimodal distribution characterized by a reduced amount of sand (20 % less in weight, Run R3 in Table 1 and Fig. 4), and two nearly uniform mixtures characterized by a mean diameter of 1 mm and 9 mm, respectively Run R1 and Run R2 in Table 1 and Fig. 4. These different mixtures are investigated with the aim of exploring the

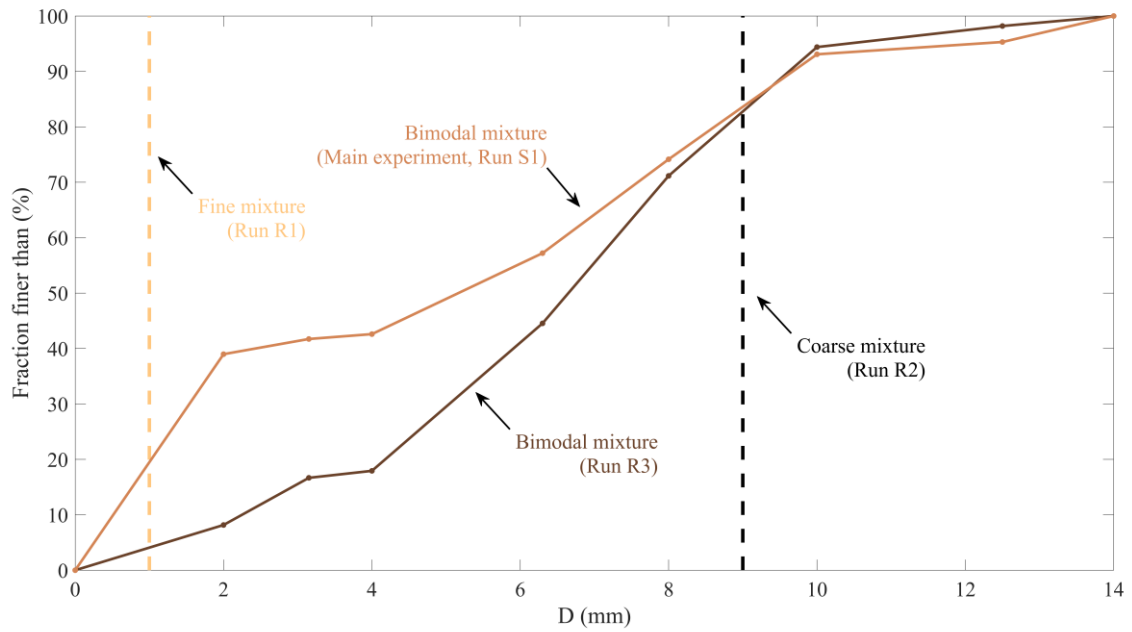


effect of grain size heterogeneity on the behaviour of the deposit. Moreover, we carry out a supplementary experiment (Run S1 in Supplement) that consists in feeding the 18 % steep channel directly using the bimodal mixture of the main experiment.
 145 Input liquid and solid discharge values are kept constant for each run.

The main experiment and Run S1 are characterized by a transport stage τ^*/τ_{CR}^* close to the unit, where τ^* is the mean Shields stress and τ_{CR}^* the critical Shields stress. We calculate the mean Shields stress as $\tau^* = \frac{\tau}{g(\rho_s - \rho)D_{84}}$, where bed shear stress is approximated under the assumption of uniform flow as $\tau = \rho u_*^2$, ρ is water density and $u_* = \sqrt{ghS}$ is the bed shear stress velocity, with h equal to water level, S being the channel slope, g is acceleration due to gravity, ρ_s is sediment density and
 150 D_{84} is the 84th percentile particle diameter. The critical shear stress is considered slope dependent and formulated following Recking et al. (2008) as $\tau_{CR}^* = 0.15 S^{0.275}$. The overall experimental conditions are shown in Table 1.

<i>Main Experiment</i>	<i>Reference experiments</i>	<i>Supplementary experiment</i>
$Q_l = 0.45 \text{ l s}^{-1}$	<ul style="list-style-type: none"> • Varying grain size distribution : <ol style="list-style-type: none"> 1) Run R1: Uniform fine 2) Run R2: Uniform coarse 3) Run R3: Bimodal with a reduced fine fraction 	<ul style="list-style-type: none"> • Without storage area: <ol style="list-style-type: none"> 4) Run S1
$Q_s = 80 \text{ g s}^{-1}$		
$C = 6.7 \%$		
$Fr = 2.85$		
$H / D_{84} = 0.70$		
$\tau^* = 0.08$		
$\tau_{cr}^* = 0.09$		
$\tau^* / \tau_{cr}^* = 0.89$		
Bimodal grain size distribution		

Table 1: Experimental conditions.



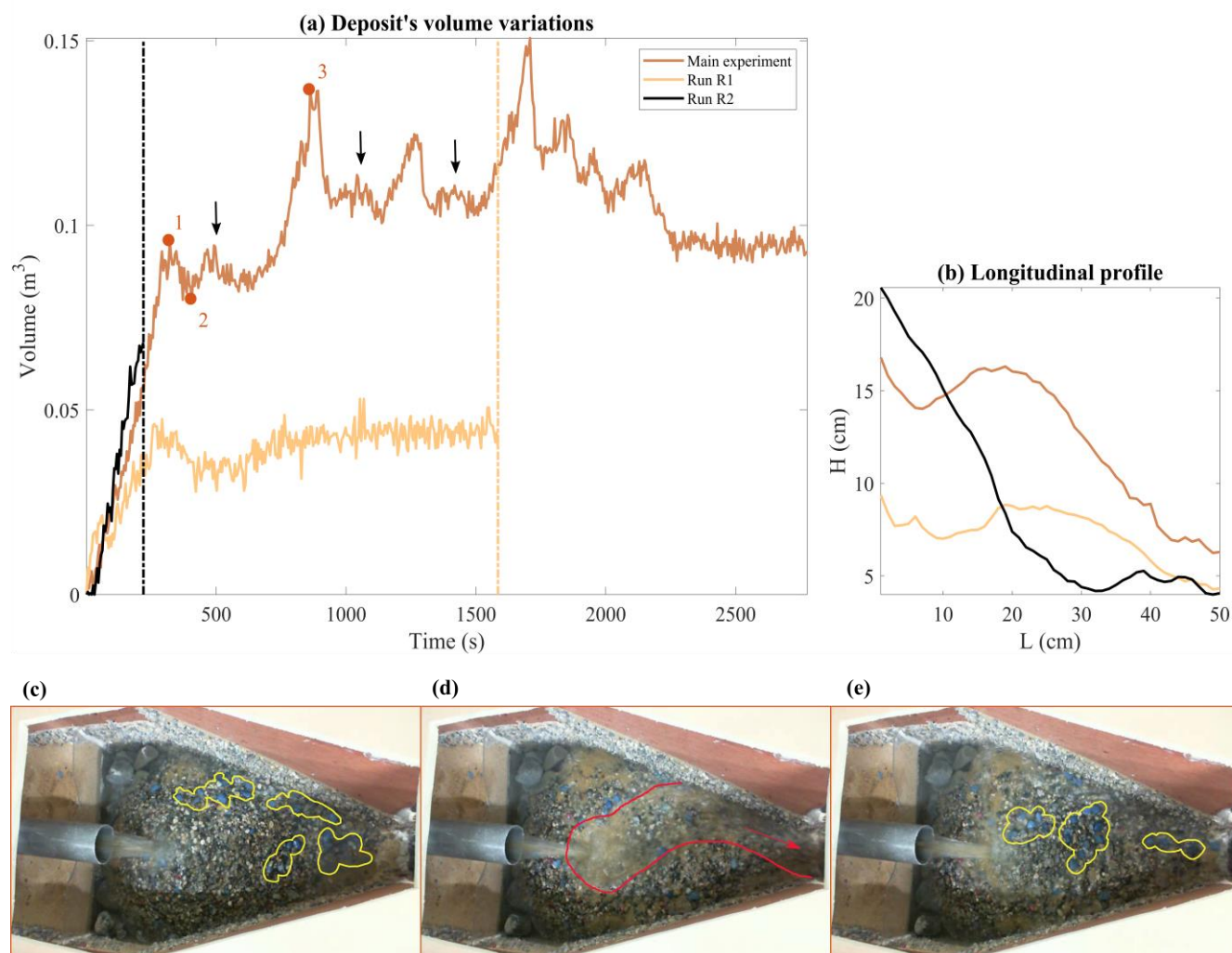
155 Figure 4: Grain size distribution of the different sediment mixtures used in the experiments.



3 Results

3.1 Dynamics of the deposit in the storage area

160 The temporal variation of the deposit's volume detected using the Kinect Camera measurements during the Main Experiment is shown with the brown curve on Fig. 5a, while the mechanisms involved in its evolution are investigated through looking at an associated video (Video 1 in the Supplement) and selected images (Fig. 5). During the first minutes (about 300 s), the flow is characterized by a limited transport capacity, which results in a nearly total deposition with no sediments reaching the downstream channel. The water flow mainly bypasses the deposit on the sides, although some infiltration also occurs, as
165 attested by subsurface flows coming out of the deposit toe. However, after a while (about 5 min) the area is almost totally flooded and a large portion of the deposit is submerged (Video 1). Local failures efficiently move clusters of sediments at the front of the deposit and on the flanks, such that the deposit grows up in the vertical and horizontal direction until it approaches the connected steep channel. We observe that grains at the surface are preferentially coarse as a result of the downward percolation of finer particles (kinematic sieving, sensu (Frey and Church, 2009)). These larger grains create an armour at the
170 surface and also roll to the deposit's toe, both the processes stabilizing the whole mass (yellow bordered particles in Fig. 5c). At this stage, the aggradation reaches its first peak (point 1 in Fig. 5a) when a significant surface water flow forms, which increases the flow-induced stresses on the deposit surface and causes armour breaking. Particles start to be transported *en masse* over a slope made of sand, which leads to the formation of active channels that transports large amounts of sediments to the downstream main channel (point 2 in Fig. 5a and red bordered area in Fig. 5d). After a first large release of material,
175 sediment bars form and stabilize the deposit (plateau that nearly lasts 300 s after point 2 in Fig. 5a). During this intermediate phase, small (but still significant) amount of sediments can be occasionally released to the channel as a result of local destabilizations (see black arrows in Fig. 5a), until a new aggradation phase begins due to a decreased transport capacity. The deposit reaches again a peak in volume with a heavily armoured surface (point 3 in Fig. 5a and Fig. 5e) before a second brutal destabilization occurs. We observe these alternating aggradation and erosion phases until the end of the run. Erosion's intensity
180 is materialised by the high gradient of the falling limb that characterizes each peak in the curve, which tells us about the volume evacuated and the velocity of the process (Fig. 5a). The last 1000 s of the experiment are characterized by a generalized depletion of material due to the saturation of the storage area.



185 **Figure 5:** (a) results from the Kinect Camera for the three runs. The volume variation of the deposit is shown versus time. The two
 vertical dotted lines show the end of the runs characterized by a uniform mixture. The black arrows indicate the sediment releases
 occurring during after the larger destabilizations and before the following aggradation phase. The orange dots with the associated
 number refer to the images presented below: the frames of the video recording represent the steps of the cyclic behaviour experienced
 by the storage area, with: (c) aggradation phase of the deposit and armouring phase at its maximum; (d) sediment pulse to the
 190 channel following the destabilization of the deposit with sand no more hidden but exposed to the flow; (e) new armouring phase. The
 yellow bordered particles form the surface armour, while the red bordered area shows the destabilized masse. (b) Comparison
 between the longitudinal profiles of the deposit for the three experiments when the aggradation phase is at its maximum. The profile
 is the result of the intersection between the deposit and a plane normal to the storage area's base and parallel to the channel.

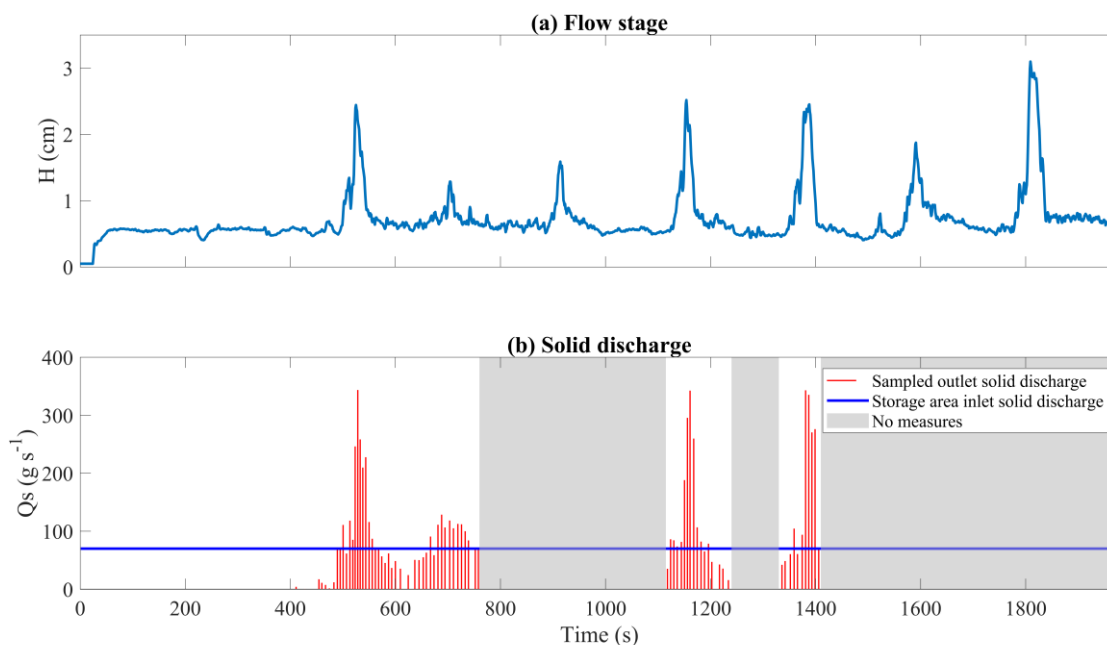
195 Interestingly, we find that the alternating behaviour as described above no longer occurs when using uniform sediment
 mixtures. The experiment using the mixture of sand (Run R1) first exhibits an aggradation phase during the first 250 s (cream-
 coloured curve in Fig. 5a) but sand quickly reaches the inlet section of the channel and the storage area starts to release
 sediments with a mean solid discharge of 156 g s^{-1} , before reaching an equilibrium with the inlet solid discharge (see Video
 2 in Supplement). The plateau in the cream-coloured curve of Fig. 5 indicates that an equilibrium phase is achieved with no



significant deposition or erosion. The experiment carried out with the coarse mixture (Run R2) leads to the formation of a steep pile in front of the injection tube. As the mobility of the grains is low, the deposit grows quickly in the vertical direction and reaches the height of the injection tube long before approaching the channel inlet. Other than for the interlocking effect of the particles, the video recording (see Video 3 in Supplement) clearly shows that the high permeability of the mixture causes the water to fully infiltrate, leading to nearly dry flow conditions at the surface (no surface flow). We observe the same behaviour in Run R3 using a bimodal mixture characterized by a low percentage of sand (around 10 % by weight, Fig. 4), whose video recording is presented in Supplement (Video 4) and where the deposit shows a strong stability and no pulses are generated. The different mobility of the three mixtures presented here is materialized by the longitudinal profile computed for each experiment during the maximum extension of the deposit (Fig. 5b). Sand easily reaches the inlet section of the channel and particles are washed away by the flow by preventing the deposit to grow in volume (cream-coloured curve in Fig. 5b). The coarse material is on the other side of the spectrum as the stability of the mixture allows the deposit to reach a 66 % longitudinal gradient (burgundy curve in Fig. 5b). In between these two conditions, the deposit made of the bimodal mixture is able to develop radially thanks to local destabilizations that spread material towards the channel (beown curve in Fig. 5b). Based on these observations, we advance that, in our experiments, the ability of the deposit to experience alternating phases of storage and erosion with the generation of sediment pulses is controlled by the presence of sand and their percolation. The processes potentially involved are discussed in *Sect. 4.1*.

3.2 Sediment pulse's propagation in the downstream channel

We investigate the propagation and physical characteristics of the sediment pulses with a specific experiment focused on the channel having the boundary conditions of the Main Experiment (see Table 1). We use the middle section's ultrasonic and geophone sensors, as well as the hand-made measurements of sediment flux and grain size distribution at the channel outlet. After the time shifting procedure (see *Sect. 2.1*), we find a clear correlation between flow stage and solid discharge measurement (Fig. 6): the passage of solid discharge pulses in the downstream channel is materialized by distinct peaks of about 60 s in the flow stage measurement time series (Fig. 6a). The biggest peaks are associated with a solid discharge of about 340 g s^{-1} (Fig. 6b), which is up to four times larger than the prescribed solid input of 80 g s^{-1} , and a sediment concentration that reaches 26.8 % in volume. The magnitude of the sediment pulses is controlled by the dynamics of the upstream storage area, as confirmed by the supplementary experiment (run S1 in Supplement and Video 5) in which we feed the 18 % steep channel directly with the same bimodal sediment mixture and observe no significant solid discharge fluctuations. The second sampled solid discharge peak around $t = 700 \text{ s}$ is smaller than the others as being the result of a local destabilization occurring just before a fully developed aggradation phase (see *Sect. 3.1*). Given the different genesis compared to the others, and a mean solid discharge almost equal to the prescribed solid input ($Q_S = 84 \text{ g s}^{-1}$), this second sediment release is not considered here as a sediment pulse.



230 **Figure 6: In-channel measurement time series of flow stage and solid discharge. Panel (a) shows flow stage as measured in the middle section. Panel (b) shows outlet solid discharge (red bars) as compared with inlet solid discharge (blue horizontal line).**

Sediment pulses are all characterized by the same composition (Fig. 7a): a front made of the coarsest fraction of the sediment mixture, a body that exhibits a predominance of sand and a tail characterized by a wide grain size distribution (Fig. 7b). This varying grain size distribution mainly results from the processes that occur in the storage area. The front made of the coarsest particles constituting the deposit surface ($D_{84} = 12.12 \text{ mm}$ in average from all front's samples) is inherited from the coarser grains being the first ones to be destabilized in the storage area. These coarser grains always precede the peak of solid discharge, and are materialized in the flow stage measurements by a small bump preceding the main pulse peak (Fig. 6a). On the opposite, the sand, which is initially hidden below the surface in the storage area, only emerge and is transported towards the channel when the bulk mass is destabilized. This large destabilization constitutes the flow stage peak, which exhibits finer grains ($D_{84} = 7.43 \text{ mm}$) and the highest concentration of sand (33 % by weight). The falling limb of the sediment pulse is composed of a wider grain size distribution ($D_{84} = 7.85 \text{ mm}$) with a high percentage of sand as well (40 % by weight), but with a decreased solid discharge as a result of the next aggradation phase starting to store sediments in the storage area. This peculiar composition is absent in the small solid discharge peak, where all the samples exhibit an average $D_{84} = 8.63 \text{ mm}$ with little inter-samples variations.

245 The video recorded one meter upstream of the middle section (see Video 6 in Supplement) allows us to characterize the transport mechanics associated with each part of the pulse. The pulse's front exhibits typical bedload dynamics with grains saltating, rolling and sliding on the bed (see the first 15 s in Video 6). The coarsest fraction occasionally gets stuck and forms small lateral clusters, consistent with transport for these large grain sizes occurring near the threshold of motion (see Sect. 2.2).



250 These bedforms are ephemeral since sudden impacts of grains can destroy their structure incorporating them in the main flow,
causing the motion of the biggest elements constituting the front to be quite intermittent. The pulse body is conversely
characterized by an enhanced mobility. Our instrumental equipment does not allow us to deeply investigate the nature of the
interactions occurring in this dense granular flow (i.e. collisional or frictional, sensu (GDR MiDi, 2004)), but an important role
in the transition between the dynamics of the front and that of the body seems to be played by the sand input, since the change
in mobility arises when fine particles enter the channel (around $t = 0:0:22$ in Video 6). Although the grain size distribution
255 is mainly imposed by the storage area, the pulse's body is also subject to in-channel grain sorting: fine sediments percolate to
the subsurface while bigger grains are pushed upward and roll over them. Despite having the same size, we observe that the
velocity of these elements is almost doubled compared to the particles constituting the front, and we advance that size
segregation is the driving mechanism for this enhanced mobility. It's worth noting that as a result of this process, a portion of
the coarse upper layer of the body can eventually move ahead and reach the already developed front before it reaches the outlet
260 section. That's why the first samples exceeding a value of 200 g s^{-1} of each sediment pulse, despite being considered part of
the pulse's body, are characterized by a consistent portion of coarse grains. As the solid concentration decreases, the tail of the
sediment pulse is back to a saltation dynamics ($t = 0:0:35$ in Video 6). Compared to the front, which has comparable solid
discharge values, the tail of the pulse is also composed of fine grains. As a consequence, thanks to an enhanced transport
capacity (Wilcock et al., 2001; Curran and Wilcock, 2005), the coarsest fraction of the mixture moves relatively fast. As
265 expected, this varying dynamics is missing for the second solid discharge peak, which exhibits a constant bedload dynamics
(see Video 7 in Supplement).

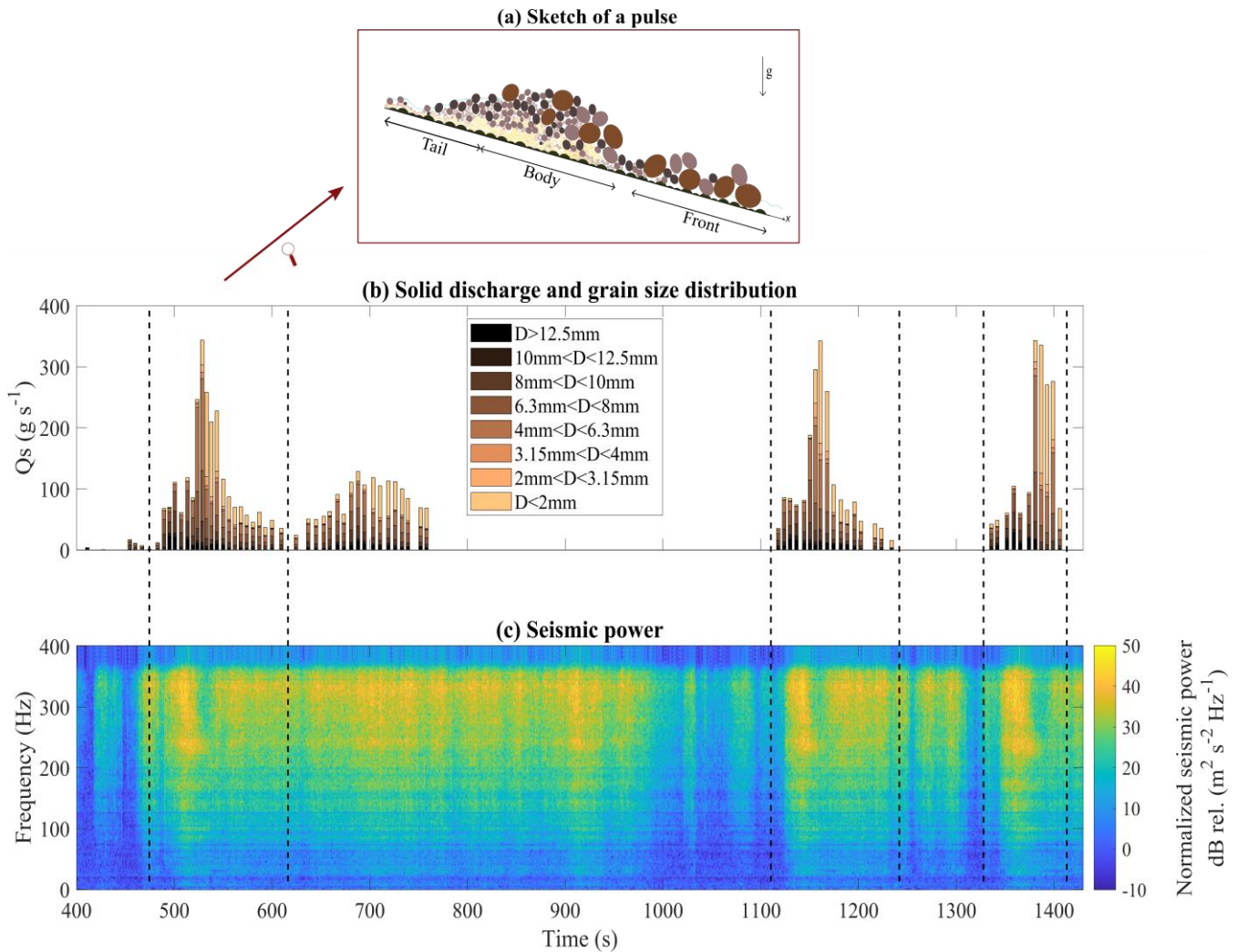


Figure 7: (a) Sketch of the sediment pulse. It can be divided in three parts: a front, a body and a tail. (b) The four sampled pulses and the small solid discharge peak are presented with their grain size distribution. Each coloured bar refers to the particle diameter displayed in the legend, while the bar length is proportional to the percentage in weight of the related particle size. (c) Seismic power detected in the middle section of the flume. The seismic power is normalized with the mean seismic power computed under no sediment transport conditions, and it is shown as a function of time and frequency, where different colours refer to different level of power.

270

275 3.3 Pulse-induced seismic motion

The passage of sediment pulses is associated with significant increases in seismic power over the whole frequency range, with the highest variations occurring above 200 Hz and being of about 30 dB (Fig. 7c, e.g. $t = 500$ s to $t = 1000$ s and $t = 1100$ s to $t = 1450$ s). Comparing the outlet solid discharge samples and the spectrogram (Fig. 7) we observe that seismic power varies considerably during the sediment pulse. Highest mean power always corresponds to the passage of the front,



280 while the body and the tail are comparatively associated with much lower values (respectively -9 dB and -6 dB compared
to the front). We verify that highest seismic power is indeed exclusively due to the passage of the pulse's front thanks to video
recordings, on which we observe that (i) most of the channel is occupied by the front and the sediment pulse body is not yet
present when the peak of seismic power is reached, and (ii) seismic power starts decreasing when front's particles get out of
the channel. Similarly, the seismic signature of the second solid discharge peak is characterized by a high level of seismic
285 power above 200 Hz, but as opposed to that of sediment pulses, seismic power is proportional to solid discharge, with higher
seismic power in the 200 – 300 Hz frequency range during the passage of higher solid discharge.

4 Discussion

4.1 The control of sand on the destabilization of sediment accumulation zones

This experimental set-up has been designed to investigate if a self-formed deposit could generate sediment pulses for a
290 downstream channel. We find that the bimodal deposit (Main experiment) exhibits a pulsating behaviour, i.e. self-induced
alternating phases of storage and release of sediments under steady external forcing. We suggest that a key role in this dynamics
is played by sand and its downward percolation. While kinematic sieving stabilizes the deposit during the aggradation phase
through building a coarse armour on the surface as observed in alluvial beds (Recking et al., 2009; Bacchi et al., 2014), the
presence of sand in the subsurface not only triggers but also enhances *en masse* erosion. We link the triggering mechanism to
295 a decrease in the deposit's hydraulic conductivity: when sand moves downward in the mixture, it fills the interstices between
grains and obstruct the subsurface water flow; as water cannot infiltrate, a surface flow develops and starts increasing shear
stresses on the particles constituting the armour, which is consequently prone to instability. The effect of fines on the hydraulic
conductivity of a sediment deposit and its failure has been investigated by Hu et al. (2017, 2018) with flume experiments on
the initiation of flow-like landslides. The authors show that the low hydraulic conductivity of mixtures rich in fines (called in
300 the papers as “small particles” to underline their non-cohesive nature) promotes pore pressure's build-up and the consequent
failure of the granular deposit. Similarly, fines' availability has been proposed as a factor able to lower the threshold of debris
flow initiation from loose sediment deposit for increasing pore water pressure (Baer et al., 2017). Since our experimental
equipment does not allow to estimate pore pressure, we cannot conclude about its potential increase near failure, but the video
recording (Video 1 in Supplement) makes us hypothesize that surface water flow exerts a major control on the destabilization
305 process.

Then, once destabilized, we propose that large parts of the deposit fail *en masse* thanks to the percolated sand that acts as a
carpet over which the overlying grains slide. This “granular lubrication” effect has been reported in previous works, where
small particles are shown to increase the run-out length of granular avalanches (Linares-Guerrero et al., 2007; Phillips et al.,
2006) and the mobility of granular column (Lai et al., 2017). Interestingly, Hu et al. (2017) wonder if the viscous interface
310 between water and small particles could affect the flow-sliding: our observations on granular lubrication can be seen as
complementary in reinforcing their intuition. The experiments using the uniform coarse material and the bimodal mixture



characterized by a low fraction of sand (Run R2 and Run R3, respectively) support these hypothesis as for equal boundary conditions the deposit shows a much inhibited mobility without any releases to the channel, even with increased water discharge (see Video 8 in Supplement).

315 We emphasize that the destabilization develops near the deposit's surface also thanks to other experiments (not presented in this paper) where we observe the same processes in deposit's formation and destabilization even if basin's surface is characterized by an enhanced roughness (big particles are randomly glued to the horizontal platform). This observation confirms the results of Lajeunesse et al. (2004), which show that the roughness of the underlying ground has a negligible impact on the dynamics of a spreading dry granular mass. Moreover, this further suggests that the specifics of the experimental
320 setup have a minor influence on our observations.

Although the processes that drive the massive failure of sediment accumulation zones may be many, the presence of sand seems to be the common denominator. Therefore, we propose that the granulometric composition of deposits should be carefully taken into account to assess their propensity to generate sediment pulses to downstream channels. We acknowledge that in the upper part of mountain catchments direct field measurements are often difficult to carry out, but geological maps
325 and high-resolution topographic surveys (Loye et al., 2016) can be sufficient for a diagnostic analysis as the amount of small sized fraction mostly depends on the local lithology and type of mass wasting processes involved in sediment production (e.g. fragmentation in rock avalanches (Zhang and McSaveney, 2017) and landslides (Davies and McSaveney, 2009)).

4.2 The dynamics of sediment pulse's body as set by the sand input from the storage area

330 Our experiments show that the sediment pulses travel downstream with ephemeral interaction with the bed, as the channel is completely free of sediments after the passage of the pulse's tail. Here we would like to stress how the massive input of fine particles during the upstream erosion phase influences the dynamics of the pulse. While at the beginning the sediment pulse's front is characterized by an intermittent dynamic and a reduced velocity, the motion of the biggest particles is dramatically enhanced with the body's arrival and passage. Nearly one century ago Gilbert (1914) demonstrated that the introduction of
335 fine particles could enhance the transport efficiency of a mixture, and many works investigated this process experimentally (Wilcock et al., 2001; Curran and Wilcock, 2005), but only recent experimental studies underline the role played by size segregation (Recking et al., 2009; Bacchi et al., 2014; Dudill et al., 2018; Chassagne et al., 2020). If Bacchi et al. (2014) and Dudill et al. (2018) show that fines enhance the mobility of big particles by smoothing the surface where they move, by modelling the process Chassagne et al. (2020) propose that after percolation fines can create a "conveyor belt" transporting at
340 higher velocity the overlying coarse grains. Although the authors showed that an exclusive "conveyor belt" contribution on the increased mobility of larger grains implies a net separation between the two main sizes, which is missing in our experiments since particles are quite mixed on the surface, from the video recording big particles appear to be passively transported downstream over a fast layer of small grains (blue pebbles over a yellowish carpet from $t = 0:0:25$ to $t = 0:0:32$ in Video 6). These observations make us think that, rather than hydrodynamics or gravity-driven processes, the efficiency with which



345 the pulse's body is digested by the channel without leaving any trace mainly depends on the capability of fine particles to carry
coarser particles as a result of kinematic sorting.

4.3 Similarities with debris flow events

Although the experiments presented in this paper do not specifically concern debris flows according to classical criteria that
rely on sediment concentration (the maximum sediment concentration of our pulses does not exceed the commonly adopted
350 threshold of 50 % by volume) and driving forces involved (the channel's slope does not allow a gravity-driven mass
movement), sediment pulses' dynamics exhibits remarkably similar characteristics to those of stony debris flows (Takahashi,
2014). A first similarity consists in the granulometric composition: a front made of boulders, a body characterized by a wide
grain size distribution and a much more diluted tail (Iverson, 1997; Stock and Dietrich, 2006). To our knowledge this feature
has been exclusively associated with processes occurring in the transportation zone such as in-channel size segregation
355 (Iverson, 1997). Although we observe this latter process as well, our experimental work shows that a selective entrainment of
grains also occurs in initiation zones, which can then have a significant role for influencing the textural composition of debris
flows. Given the difficulty of carrying out direct field observations initiation zones (Berti et al., 1999; Imaizumi et al., 2006;
McCoy et al., 2012; Loye et al., 2016), we suggest that this kind of experimental set-up could be useful for investigating the
mechanisms of both debris flow initiation and transportation.

360 Our findings also confirm the hypothesis of Kean (2013) for which the presence of a sediment accumulation zone can play a
key role in the triggering of cyclic debris flow surges resulting from alternate aggradation and mass failure phases. In particular,
the authors point out that the regressive instabilities (sensu (Zanuttigh and Lamberti, 2007)) of those debris flows that are
generated by water runoff (i.e. runoff-induced debris flows) may develop thanks to the presence of local low-slope sections of
the channel where sediments can temporally be stored and then suddenly released. Channel portions characterized by a local
365 decrease in sediment transport capacity, referred to as "sediment capacitors", can turn steady or quasi-steady supply conditions
into discrete debris flow pulses. In modelling this phenomenon, Kean et al. (2013) use a uniform grain size distribution but
acknowledge that a wide grain size distribution might affect surge characteristics. Our experiments corroborate this
consideration and further stress how the granulometric composition of deposits must be considered a key driver for debris
flows' pulsating behaviour.

370 4.4 Links between pulse's dynamics and seismic noise

We observe a complex seismic response to sediment pulses, characterised by a non-unique dependency between seismic power
and sediment transport characteristics such as grain size and sediment flux. Highest seismic power is caused by the propagating
front, consistent with the presence of larger grains causing more energetic impacts (Tsai et al., 2012). However, reduced
seismic power is observed during the passage of the pulse body, although this latter is associated with the highest sediment
375 flux, a parameter which is often aimed at being inverted from the seismic signal (Tsai et al., 2012; Bakker et al., 2020). Using
the prediction of Tsai et al. (2012) that seismic power approximately scales as $D_{94}^3 q_s$, where D is the particle diameter and q_s



is sediment flux, we find that reduced seismic power (on the order of 9 dB) between the front and the body of the pulse cannot be explained solely by changes in D and q_s , since D decreasing by about a factor of 0.7 ($D_{94} = 12.93 \text{ mm}$) for the front compared to $D_{94} = 9.32 \text{ mm}$ for the body) and q_s increasing by about a factor of 4 (from 80 g s^{-1} for the front up to 380 340 g s^{-1} for the body) would yield approximately constant seismic power, which is not observed. Since seismic records show a reduced sensitivity to this component of the pulse, which in fact accounts for the largest fraction of the sediment flux, the capability of existing models of reliably inverting solid discharge from seismic power is questioned for this kind of transport processes.

Since our sediment pulses show similarities with debris flows (see *Sect. 4.3*), we find appropriate to compare our observations 385 also with expectations from theories of debris flow-induced seismic noise. Conveniently, our experimental set-up allows us to study the seismic responses of the different parts of the pulse (front, body, and tail) separately, as opposed to the field where all parts of the pulse can potentially contribute to the overall measured seismic noise. Our observations are consistent with most of field surveys and models, for which the front (sometimes referred to as snout) generates a stronger seismic power than the following flow as it carries the largest clasts (Arattano and Moia, 1999; Lai et al., 2018; Coviello et al., 2019; Farin et al., 390 2019; Allstadt et al., 2020). However, the relationship between seismic noise and flow thickness is contrasting. While some observations show a good correlation between flow thickness and fluctuating basal stresses (Allstadt et al., 2020) and some models reveal no or rare direct dependence (Lai et al., 2018; Farin et al., 2019), our experiments show a clear negative correlation since pulse's body is characterized by the peak of flow stage (Fig. 6). According to Cole et al. (2009) and Allstadt et al. (2020), this could be explained by its high solid concentration. Indeed, they observe a negative correlation between bulk 395 density and seismic noise, and therefore propose that more agitated flows are “louder” than denser and plug-like flows. This interpretation would be also consistent with the increase of seismic noise associated to the pulse's tail, which is again much more diluted than the body.

Further work remains to be conducted in order to fully unravel the control of the pulse's internal dynamics on the generated seismic noise. In particular, it appears as essential to more quantitatively investigate the effect of grain sorting, which likely 400 plays a crucial role through pushing upward the biggest particles, thus preventing them from directly impacting the bed and reducing their contribution to seismic noise. This would be consistent with the field observations of Kean et al. (2015), who suggest that the presence of a sediment layer over the bedrock can strongly damp the seismic signal generated by a debris flow. Detailed analysis of particle impact velocities, rates and applied forces across the different grain sizes and the different pulses components would help further addressing these aspects.

405



5 Conclusions

We carry out flume experiments characterized by an original set-up where instead of feeding the flume section directly as usually done, we supply with liquid and solid discharge a low slope storage zone acting like a natural sediment accumulation zone and connected to a 18 % steep channel. The experiments reveal that:

- 410 1) under constant feeding conditions, when a bimodal grain size distribution with a high fraction of sand is used, the storage area is subject to alternating aggradation and erosion phases. The high morphological mobility of the deposit is due to several autogenic processes, but the presence of sand appears to play a key role. In particular, if during the aggradation phase grain sorting enhances the stability of the deposit in coarsening its surface thanks to the downward percolation of the fine particles, we propose that the infilling of the subsurface with fine material contributes to the
- 415 destabilization of the deposit by two means: (i) it reduces the hydraulic conductivity of the deposit and causes the formation of a significant surface water flow that in turn increases the stresses over the armoured layer, (ii) it acts like a smooth carpet where the coarser grains slides *en masse*.
- 420 2) the erosion phases correspond to the generation of sediment pulses towards the downstream channel. The evolution of the sediment deposit affects not only the magnitude of the sediment pulses, but also their rheology and dynamics. Each sediment pulse can be divided in three different components as follows: a front having a low solid discharge made of the coarsest fraction of the sediment mixture, inherited by the destabilization of deposit's surface; a body that corresponds to the peak of solid discharge, composed of a high concentration of sand coming from deposit's subsurface; a tail characterized by a low solid discharge and a wide grain size distribution, with sediments still transported while the next aggradation phase starts to develop in the storage area.
- 425 3) pulses in sediment transport can be detected by seismic measurements. We find that the sediment pulse's front dominates the overall seismic noise. However, we report a complex link between seismic power to the different parts of the sediment pulse, which questions the validity of current models and theories to such transport dynamics. Further work is needed to unravel the role of the different pulse's geometrical and dynamical parameters on the generated seismic noise.
- 430 From a practical point of view, these results have strong implications in natural risk management. First, we show that the proximity of upstream sediment accumulation zones must be considered a potential source of sediment pulses for mountain rivers, regardless of bed sediments' availability. Second, since the grain size distribution is shown to have a direct influence on the mobility (i.e. stability) of debris deposits, we challenge the classical approach for which the *sediment context* of mountain catchments is merely reduced to an available volume and hydrological conditions are considered the main factor
- 435 controlling the activation of external sediment supply. Instead, the granular conditions of deposits that are coupled with mountain streams or stored in low slope portion of the channel should be taken into account for assessing the occurrence and dynamics of such dramatic transport events. Finally, our seismic findings challenge the application of current theoretical frameworks to invert bedload flux from the seismic noise associated with this kind of transport processes.



440 *Author contributions:* MP, AR and FG designed the laboratory experiments. MP developed the flume and HB led the installation of the instrumental equipment. MP carried out the experiments with the help of HB. MP interpreted the results, with input from FG, AR and HB. MP led the writing of the paper, and FG and AR revised and contributed to it.

Competing interests: The authors declare that they have no conflict of interest.

445

Data availability: The datasets analysed during the current study are available and temporary shared on this link:

<https://www.dropbox.com/sh/n3oqyl06csmnpg/AABnNuhwb1RZIAhSRFt6EbEba?dl=0>

In case of acceptance we plan to give access to all data through the data repository platform Zenodo with an associated Digital Object Identifier (DOI).

450

Video supplement: The videos used for the analysis are temporary available on this link:

<https://www.dropbox.com/sh/ctyxz64hn0di41s/AAAgvoEkXihVE44norGPC-E8a?dl=0>

The DOI's generation through the AV Portal of TIB Hannover is in progress.

455 *Acknowledgements:* This research is funded by the French Agence nationale de la recherche, project ANR-17-CE01-0008. We acknowledge the support of the INRAE Research Centre of Grenoble for the laboratory and the instrumental equipment. We thank Christian Eymond-Gris, Frédéric Ousset, and Xavier Ravanat for the technical support in the development of the flume. We thank Maarten Bakker for helping in the analysis of the seismic data.

460 **References**

Allstadt, K. E., Farin, M., Iverson, R. M., Obryk, M. K., Kean, J. W., Tsai, V. C., Rapstine, T. D., and Logan, M.: Measuring Basal Force Fluctuations of Debris Flows Using Seismic Recordings and Empirical Green's Functions, *J. Geophys. Res. Earth Surf.*, 125, <https://doi.org/10.1029/2020JF005590>, 2020.

465 Arattano, M. and Moia, F.: Monitoring the propagation of a debris flow along a torrent, *Hydrological Sciences Journal*, 44, 811–823, <https://doi.org/10.1080/02626669909492275>, 1999.

Bacchi, V., Recking, A., Eckert, N., Frey, P., Piton, G., and Naaim, M.: The effects of kinetic sorting on sediment mobility on steep slopes: GRAIN SORTING ON STEEP SLOPES, *Earth Surf. Process. Landforms*, 39, 1075–1086, <https://doi.org/10.1002/esp.3564>, 2014.

470 Badoux, A., Andres, N., and Turowski, J. M.: Damage costs due to bedload transport processes in Switzerland, *Nat. Hazards Earth Syst. Sci.*, 14, 279–294, <https://doi.org/10.5194/nhess-14-279-2014>, 2014.



- Baer, P., Huggel, C., McArdell, B. W., and Frank, F.: Changing debris flow activity after sudden sediment input: a case study from the Swiss Alps, *Geology Today*, 33, 216–223, <https://doi.org/10.1111/gto.12211>, 2017.
- Bakker, M., Gimbert, F., Geay, T., Misset, C., Zanker, S., and Recking, A.: Field Application and Validation of a Seismic Bedload Transport Model, *J. Geophys. Res. Earth Surf.*, 125, <https://doi.org/10.1029/2019JF005416>, 2020.
- 475 Benda, L. and Dunne, T.: Stochastic forcing of sediment routing and storage in channel networks, *Water Resour. Res.*, 33, 2865–2880, <https://doi.org/10.1029/97WR02387>, 1997.
- Berti, M., Genevois, R., Simoni, A., and Tecca, P. R.: Field observations of a debris flow event in the Dolomites, *Geomorphology*, 29, 265–274, [https://doi.org/10.1016/S0169-555X\(99\)00018-5](https://doi.org/10.1016/S0169-555X(99)00018-5), 1999.
- Bovis, M. J. and Jakob, M.: The role of debris supply conditions in predicting debris flow activity, 16, 1999.
- 480 Brummer, C. J. and Montgomery, D. R.: Influence of coarse lag formation on the mechanics of sediment pulse dispersion in a mountain stream, Squire Creek, North Cascades, Washington, United States: LAG INFLUENCE ON PULSE DISPERSION, *Water Resour. Res.*, 42, <https://doi.org/10.1029/2005WR004776>, 2006.
- Burtin, A., Hovius, N., and Turowski, J. M.: Seismic monitoring of torrential and fluvial processes, *Earth Surf. Dynam.*, 4, 285–307, <https://doi.org/10.5194/esurf-4-285-2016>, 2016.
- 485 Chassagne, R., Maurin, R., Chauchat, J., and Frey, P.: Mobility of bidisperse mixtures during bedload transport, *Phys. Rev. Fluids*, 5, 114307, <https://doi.org/10.1103/PhysRevFluids.5.114307>, 2020.
- Cole, S. E., Cronin, S. J., Sherburn, S., and Manville, V.: Seismic signals of snow-slurry lahars in motion: 25 September 2007, Mt Ruapehu, New Zealand, *Geophys. Res. Lett.*, 36, L09405, <https://doi.org/10.1029/2009GL038030>, 2009.
- Comiti, F. and Mao, L.: Recent Advances in the Dynamics of Steep Channels, in: *Gravel-Bed Rivers*, edited by: Church, M., Biron, P. M., and Roy, A. G., John Wiley & Sons, Ltd, Chichester, UK, 351–377, <https://doi.org/10.1002/9781119952497.ch26>, 2012.
- Comiti, F., Cadol, D., and Wohl, E.: Flow regimes, bed morphology, and flow resistance in self-formed step-pool channels: FLOW RESISTANCE IN STEP-POOL CHANNELS, *Water Resour. Res.*, 45, <https://doi.org/10.1029/2008WR007259>, 2009.
- 495 Cook, K. L., Andermann, C., Gimbert, F., Adhikari, B. R., and Hovius, N.: Glacial lake outburst floods as drivers of fluvial erosion in the Himalaya, *Science*, 362, 53–57, <https://doi.org/10.1126/science.aat4981>, 2018.
- Coviello, V., Arattano, M., Comiti, F., Macconi, P., and Marchi, L.: Seismic Characterization of Debris Flows: Insights into Energy Radiation and Implications for Warning, *J. Geophys. Res. Earth Surf.*, 124, 1440–1463, <https://doi.org/10.1029/2018JF004683>, 2019.
- Cui, Y. and Parker, G.: Numerical Model of Sediment Pulses and Sediment-Supply Disturbances in Mountain Rivers, *J. Hydraul. Eng.*, 131, 646–656, [https://doi.org/10.1061/\(ASCE\)0733-9429\(2005\)131:8\(646\)](https://doi.org/10.1061/(ASCE)0733-9429(2005)131:8(646)), 2005.
- 500 Cui, Y., Parker, G., Lisle, T. E., Gott, J., Hansler-Ball, M. E., Pizzuto, J. E., Allmendinger, N. E., and Reed, J. M.: Sediment pulses in mountain rivers: 1. Experiments: SEDIMENT PULSE EXPERIMENTS, *Water Resour. Res.*, 39, <https://doi.org/10.1029/2002WR001803>, 2003.
- 505 Curran, J. C. and Wilcock, P. R.: Effect of Sand Supply on Transport Rates in a Gravel-Bed Channel, *J. Hydraul. Eng.*, 131, 961–967, [https://doi.org/10.1061/\(ASCE\)0733-9429\(2005\)131:11\(961\)](https://doi.org/10.1061/(ASCE)0733-9429(2005)131:11(961)), 2005.



- Davies, T. R. and McSaveney, M. J.: The role of rock fragmentation in the motion of large landslides, *Engineering Geology*, 109, 67–79, <https://doi.org/10.1016/j.enggeo.2008.11.004>, 2009.
- Dudill, A., Lafaye de Micheaux, H., Frey, P., and Church, M.: Introducing Finer Grains Into Bedload: The Transition to a New Equilibrium, *J. Geophys. Res. Earth Surf.*, 123, 2602–2619, <https://doi.org/10.1029/2018JF004847>, 2018.
- 510 Farin, M., Tsai, V. C., Lamb, M. P., and Allstadt, K. E.: A physical model of the high-frequency seismic signal generated by debris flows, *Earth Surf. Process. Landforms*, 44, 2529–2543, <https://doi.org/10.1002/esp.4677>, 2019.
- Frey, P. and Church, M.: How River Beds Move, *Science*, 325, 1509–1510, <https://doi.org/10.1126/science.1178516>, 2009.
- GDR MiDi: On dense granular flows, *Eur. Phys. J. E*, 14, 341–365, <https://doi.org/10.1140/epje/i2003-10153-0>, 2004.
- Gilbert, G. K.: The transportation of debris by running water, US Geological Survey, Washington, DC, 1914.
- 515 Gimbert, F., Fuller, B. M., Lamb, M. P., Tsai, V. C., and Johnson, J. P. L.: Particle transport mechanics and induced seismic noise in steep flume experiments with accelerometer-embedded tracers: Experimental Testing of Seismic Noise Generated by Sediment Transport, *Earth Surf. Process. Landforms*, 44, 219–241, <https://doi.org/10.1002/esp.4495>, 2019.
- Govi, M., Maraga, F., and Moia, F.: Seismic detectors for continuous bed load monitoring in a gravel stream, *Hydrological Sciences Journal*, 38, 123–132, <https://doi.org/10.1080/02626669309492650>, 1993.
- 520 Hu, W., Scaringi, G., Xu, Q., Pei, Z., Van Asch, T. W. J., and Hicher, P.-Y.: Sensitivity of the initiation and runout of flowslides in loose granular deposits to the content of small particles: An insight from flume tests, *Engineering Geology*, 231, 34–44, <https://doi.org/10.1016/j.enggeo.2017.10.001>, 2017.
- Hu, W., Scaringi, G., Xu, Q., and Huang, R.: Internal Erosion Controls Failure and Runout of Loose Granular Deposits: Evidence From Flume Tests and Implications for Postseismic Slope Healing, *Geophys. Res. Lett.*, 45, 5518–5527, <https://doi.org/10.1029/2018GL078030>, 2018.
- 525 Imaizumi, F., Sidle, R. C., Tsuchiya, S., and Ohsaka, O.: Hydrogeomorphic processes in a steep debris flow initiation zone: HYDROGEOMORPHOLOGY OF DEBRIS FLOW SITES, *Geophys. Res. Lett.*, 33, n/a-n/a, <https://doi.org/10.1029/2006GL026250>, 2006.
- Iverson, R. M.: The physics of debris flows, *Rev. Geophys.*, 35, 245–296, <https://doi.org/10.1029/97RG00426>, 1997.
- 530 Kean, J. W., McCoy, S. W., Tucker, G. E., Staley, D. M., and Coe, J. A.: Runoff generated debris flows: Observations and modeling of surge initiation, magnitude, and frequency, 118, 2190–2207, 2013.
- Kean, J. W., Coe, J. A., Coviello, V., Smith, J. B., McCoy, S. W., and Arattano, M.: Estimating rates of debris flow entrainment from ground vibrations: GROUND VIBRATIONS FROM DEBRIS FLOWS, *Geophys. Res. Lett.*, 42, 6365–6372, <https://doi.org/10.1002/2015GL064811>, 2015.
- 535 Lai, V. H., Tsai, V. C., Lamb, M. P., Ulizio, T. P., and Beer, A. R.: The Seismic Signature of Debris Flows: Flow Mechanics and Early Warning at Montecito, California, *Geophys. Res. Lett.*, 45, 5528–5535, <https://doi.org/10.1029/2018GL077683>, 2018.
- Lai, Z., Vallejo, L. E., Zhou, W., Ma, G., Espitia, J. M., Caicedo, B., and Chang, X.: Collapse of Granular Columns With Fractal Particle Size Distribution: Implications for Understanding the Role of Small Particles in Granular Flows, *Geophys. Res. Lett.*, 44, <https://doi.org/10.1002/2017GL075689>, 2017.
- 540



- Lajeunesse, E., Mangeney-Castelnau, A., and Vilotte, J. P.: Spreading of a granular mass on a horizontal plane, *Physics of Fluids*, 16, 2371–2381, <https://doi.org/10.1063/1.1736611>, 2004.
- Lamand, E., Piton, G., and Recking, A.: *Hydrologie et hydraulique torrentielle, étude d'un cas pratique: la Roize*, 90, 2017.
- 545 Lamb, M. P., Dietrich, W. E., and Venditti, J. G.: Is the critical Shields stress for incipient sediment motion dependent on channel-bed slope?, *J. Geophys. Res.*, 113, F02008, <https://doi.org/10.1029/2007JF000831>, 2008.
- Lee, A. J. and Ferguson, R. I.: Velocity and flow resistance in step-pool streams, *Geomorphology*, 46, 59–71, [https://doi.org/10.1016/S0169-555X\(02\)00054-5](https://doi.org/10.1016/S0169-555X(02)00054-5), 2002.
- Linares-Guerrero, E., Goujon, C., and Zenit, R.: Increased mobility of bidisperse granular avalanches, *J. Fluid Mech.*, 593, 475–504, <https://doi.org/10.1017/S0022112007008932>, 2007.
- 550 Lisle, T. E., Pizzuto, J. E., Ikeda, H., Iseya, F., and Kodama, Y.: Evolution of a sediment wave in an experimental channel, *Water Resour. Res.*, 33, 1971–1981, <https://doi.org/10.1029/97WR01180>, 1997.
- Loye, A., Jaboyedoff, M., Theule, J. I., and Liébault, F.: Headwater sediment dynamics in a debris flow catchment constrained by high-resolution topographic surveys, *Earth Surf. Dynam.*, 4, 489–513, <https://doi.org/10.5194/esurf-4-489-2016>, 2016.
- 555 Mao, L., Cavalli, M., Comiti, F., Marchi, L., Lenzi, M. A., and Arattano, M.: Sediment transfer processes in two Alpine catchments of contrasting morphological settings, *Journal of Hydrology*, 364, 88–98, <https://doi.org/10.1016/j.jhydrol.2008.10.021>, 2009.
- McCoy, S. W., Kean, J. W., Coe, J. A., Tucker, G. E., Staley, D. M., and Wasklewicz, T. A.: Sediment entrainment by debris flows: In situ measurements from the headwaters of a steep catchment: SEDIMENT ENTRAINMENT BY DEBRIS FLOWS, *J. Geophys. Res.*, 117, n/a-n/a, <https://doi.org/10.1029/2011JF002278>, 2012.
- 560 Phillips, J., Hogg, A., Kerswell, R., and Thomas, N.: Enhanced mobility of granular mixtures of fine and coarse particles, *Earth and Planetary Science Letters*, 246, 466–480, <https://doi.org/10.1016/j.epsl.2006.04.007>, 2006.
- Piton, G. and Recking, A.: The concept of travelling bedload and its consequences for bedload computation in mountain streams: HOW TO ACCOUNT FOR ALLOGENIC SUPPLY IN BEDLOAD TRANSPORT EQUATIONS?, *Earth Surf. Process. Landforms*, 42, 1505–1519, <https://doi.org/10.1002/esp.4105>, 2017.
- 565 Prancevic, J. P. and Lamb, M. P.: Unraveling bed slope from relative roughness in initial sediment motion: Relative roughness and incipient motion, *J. Geophys. Res. Earth Surf.*, 120, 474–489, <https://doi.org/10.1002/2014JF003323>, 2015.
- Prancevic, J. P., Lamb, M. P., and Fuller, B. M.: Incipient sediment motion across the river to debris-flow transition, 42, 191–194, <https://doi.org/10.1130/G34927.1>, 2014.
- 570 Recking, A.: Theoretical development on the effects of changing flow hydraulics on incipient bed load motion: INCIPIENT MOTION CONDITIONS, *Water Resour. Res.*, 45, <https://doi.org/10.1029/2008WR006826>, 2009.
- Recking, A.: Influence of sediment supply on mountain streams bedload transport, *Geomorphology*, 175–176, 139–150, <https://doi.org/10.1016/j.geomorph.2012.07.005>, 2012.
- Recking, A.: Relations between bed recharge and magnitude of mountain streams erosions, *Journal of Hydro-environment Research*, 8, 143–152, <https://doi.org/10.1016/j.jher.2013.08.005>, 2014.



- 575 Recking, A., Frey, P., Paquier, A., Belleudy, P., and Champagne, J. Y.: Feedback between bed load transport and flow resistance in gravel and cobble bed rivers: FEEDBACK BETWEEN BED LOAD AND FLOW RESISTANCE, *Water Resour. Res.*, 44, <https://doi.org/10.1029/2007WR006219>, 2008.
- Recking, A., Frey, P., Paquier, A., and Belleudy, P.: An experimental investigation of mechanisms involved in bed load sheet production and migration, *J. Geophys. Res.*, 114, F03010, <https://doi.org/10.1029/2008JF000990>, 2009.
- 580 Schneider, J. M., Rickenmann, D., Turowski, J. M., Schmid, B., and Kirchner, J. W.: Bed load transport in a very steep mountain stream (Riedbach, Switzerland): Measurement and prediction: BED LOAD TRANSPORT RIEDBACH, *Water Resour. Res.*, 52, 9522–9541, <https://doi.org/10.1002/2016WR019308>, 2016.
- Schumm, S. A.: *The fluvial system*, Repr., Blackburn Press, Caldwell, NJ, 338 pp., 2003.
- 585 Sklar, L. S., Fadde, J., Venditti, J. G., Nelson, P., Wyzga, M. A., Cui, Y., and Dietrich, W. E.: Translation and dispersion of sediment pulses in flume experiments simulating gravel augmentation below dams: TRANSLATION AND DISPERSION OF SEDIMENT PULSES, *Water Resour. Res.*, 45, <https://doi.org/10.1029/2008WR007346>, 2009.
- Solari, L. and Parker, G.: The Curious Case of Mobility Reversal in Sediment Mixtures, *J. Hydraul. Eng.*, 126, 185–197, [https://doi.org/10.1061/\(ASCE\)0733-9429\(2000\)126:3\(185\)](https://doi.org/10.1061/(ASCE)0733-9429(2000)126:3(185)), 2000.
- 590 Stock, J. D. and Dietrich, W. E.: Erosion of steepland valleys by debris flows, *Geological Society of America Bulletin*, 118, 1125–1148, <https://doi.org/10.1130/B25902.1>, 2006.
- Sutherland, D. G., Ball, M. H., Hilton, S. J., and Lisle, T. E.: Evolution of a landslide-induced sediment wave in the Navarro River, California, 13, 2002.
- Takahashi, T.: *Debris flow: mechanics, prediction and countermeasures*, 2. ed., CRC Press/Balkema, Boca Raton, Fla., 551 pp., 2014.
- 595 Tsai, V. C., Minchew, B., Lamb, M. P., and Ampuero, J.-P.: A physical model for seismic noise generation from sediment transport in rivers: SEISMIC NOISE FROM SEDIMENT TRANSPORT, *Geophys. Res. Lett.*, 39, n/a-n/a, <https://doi.org/10.1029/2011GL050255>, 2012.
- Welch, P.: The use of fast Fourier transform for the estimation of power spectra: A method based on time averaging over short, modified periodograms, *IEEE Trans. Audio Electroacoust.*, 15, 70–73, <https://doi.org/10.1109/TAU.1967.1161901>, 1967.
- 600 Wilcock, P. R., Kenworthy, S. T., and Crowe, J. C.: Experimental study of the transport of mixed sand and gravel, *Water Resour. Res.*, 37, 3349–3358, <https://doi.org/10.1029/2001WR000683>, 2001.
- Wohl, E. E.: *Mountain rivers revisited*, American Geophysical Union, Washington, DC, 573 pp., 2010.
- Zanuttigh, B. and Lamberti, A.: Instability and surge development in debris flows: SURGES IN DEBRIS FLOWS, *Rev. Geophys.*, 45, n/a-n/a, <https://doi.org/10.1029/2005RG000175>, 2007.
- 605 Zhang, M. and McSaveney, M. J.: Rock avalanche deposits store quantitative evidence on internal shear during runoff: Avalanche Deposits Store Shear Evidence, *Geophys. Res. Lett.*, 44, 8814–8821, <https://doi.org/10.1002/2017GL073774>, 2017.
- Zimmermann, A., Church, M., and Hassan, M. A.: Step-pool stability: Testing the jammed state hypothesis: STEP-POOL STABILITY, *J. Geophys. Res.*, 115, <https://doi.org/10.1029/2009JF001365>, 2010.